JEE Journal of Ecological Engineering

Journal of Ecological Engineering, 2026, 27(5), 323–338
https://doi.org/10.12911/22998993/216405
ISSN 2299–8993, License CC-BY 4.0

Received: 2025.12.17
Accepted: 2026.03.16
Published: 2026.04.01

Performance of innovative hybrid solar desalination system powered by using heat storage materials under a vacuum condition

Munawar Rusli[1,2*], Rofiq Iqbal[3], Suprihanto Notodarmojo[3], Mindriany Syafila[3]

[1] Doctoral Program of Environmental Engineering, Faculty of Civil and Environmental Engineering, Institut Teknologi Bandung, Jalan Ganesha No. 10, Bandung, Indonesia
[2] Department of Chemical Engineering, Politeknik Negeri Lhokseumawe, Jl. B. Aceh-Medan Km. 280, Lhokseumawe, Indonesia
[3] Department of Environmental Engineering, Faculty of Civil and Environmental Engineering, Institut Teknologi Bandung, Jalan Ganesha No. 10, Bandung, Indonesia
* Corresponding author's e-mail: munawar_rusli@pnl.ac.id

ABSTRACT

The fresh water crisis is a global issue that has threatened human life in recent years. In the areas with a lack fresh water resources, quality enhancement of saline water, the most abundant water resources in nature, by using the desalination process has become a promising solution to be used. According to ecologically friendly and sustainable effort, renewable energy-based desalination is one promising choice to address this issue. This research aimed to determine the performance of an innovative hybrid solar desalination system, which uses several materials that accelerate evaporation on the surface and store a heat, which is predicted to have significant potential for application in the desalination technology. The research consists of two parts of the experimental section that started with determining the optimum conditions for HSDS, which was conducted to determine the optimum feed water flow rate and the optimum initial feed water concentration, followed by the HSDS system performance study that was conducted to determine the effect of heat storage materials and cooling water flowrate in vacuum condition. The performance of the developed hybrid solar desalination system was quite high with hourly yield of 28.03 L/m^2 over 5 hours, and the optimum desalination efficiency of 55.42%, which was obtained at a cooling water flowrate of 4 L/minute, and the use of black gravel. The energy supplied to the system ranged from 13,064–15,506 kJ, with an energy consumption of 9,415–9,601 kJ. Meanwhile, the energy loss within the system was 3,463–6,091 kJ, or approximately 26.51–39.28% of the energy supplied to the system. Under optimum conditions, the thermal efficiency and gain output ratio (GOR) of the HSDS were 58.7% and 1.32, respectively.

Keywords: HSDS, GOR, performance, thermal efficiency, yield.

INTRODUCTION

The fresh water crisis has become a global issue in recent decades. Fresh water is a renewable resource, but human population growth and increasing exploitation of water resources mean the world's 7 billion people will face a clean water crisis in the coming years (Subramani and Jacangelo, 2015). It is predicted that approximately 70% of the global population will experience a water deficit by 2025 (Anand et al., 2021). Despite having relatively large freshwater resources (6% of the world's water reserves), Indonesia is considered a country at high risk of experiencing a water crisis. According to a report by the World Resources Institute (WRI), Indonesia is among the countries facing a high risk of water scarcity by 2040, based on the water scarcity projections (Asfahan et al., 2022). Compared to neighboring countries, such as Malaysia, the Philippines, Singapore, and even Vietnam, Indonesia's water availability remains far below average. Indonesia's piped water supply system is only capable of serving

21.8% of its total population of 270.2 million. This is the lowest service capacity in Southeast Asia (Bappenas, 2019). Therefore, the improvement efforts to address the threat of this water crisis are highly relevant and urgently required.

The water crisis is one of the most important global issues that requires serious attention, because it affects the existence of the human population on Earth. In the countries with abundant freshwater resources, the water crisis can be anticipated by improving water resource management systems, for example by optimizing the development and management of strategic water reservoirs. However, in the areas with limited water resources, one solution to the water crisis is to utilize the most abundant natural resources, namely seawater and brackish water, through a process called desalination (Pistocchi et al., 2020). Scientific studies conducted by many researchers indicate that the application of desalination technology to purify seawater and brackish water has very promising prospects for use in the efforts to reduce the rate of clean water deficit (Pistocchi et al., 2020; Raihananda et al., 2021). These desalination installations globally produce no less than 160 million m^3/day (Kumar et al., 2022), and serve as the primary water source for approximately 0.5 billion people globally (Alhaj et al., 2022). Unfortunately, Indonesia still relies on conventional water production systems, which in reality are only capable of serving 21.8–47.71% of the population (Fairuz et al., 2023). At this point, there is a gap in technological implementation that needs to be bridged by developing innovative water production systems, such as sustainable desalination systems, by maximizing the potential of national resources.

This research aimed to study the characteristics and performance of a hybrid solar desalination system (HSDS) powered by solar driven interface/thermal energy storage materials for salinity reduction in salt water. The effect of cooling water flowrate, energy analysis, and thermal efficiency of the system was also investigated. The combination of a two-way heating system (direct and indirect heating), a vacuum system, the use of heat storage materials, and the use of separated condensation system in the integrated HSDS devices constitute the innovative configuration in the hybrid solar desalination system that is being used for the first time in this study.

MATERIALS AND METHODS

The research was conducted at the Fugha Workshop in Lhokseumawe City, which has a solar energy conversion system facility with a capacity of 1800 WP, and has a work area with intense sunlight exposure and an adequate source of cooling water.

Materials

The HSDS system consists of three main units, namely the evaporator, with a heat transfer surface area of ≥ 0.25 m^2 (Munawar et al., 2022; Munawar and Majuar, 2019), and is assembled with a feed tank and condenser, as well as a solar power conversion system (Figure 1). The evaporator uses a dual heating system, consisting of direct solar heating and heating with a heater supplied with electrical energy from a solar energy conversion unit. The solar energy conversion system consists of solar panels, an inverter, and an energy storage system or battery (Isah et al., 2022; Munawar, 2022). The evaporator is also filled with solar-driven interface (SDI) or heat storage (HS) materials (Dong et al., 2022; Li et al., 2020; Raihananda et al., 2021; Nema et.al., 2025), consisting of black gravel, quartz sand, and black sand. A vacuum system is used to transport vapor from the evaporator to the condenser (Munawar and Majuar, 2019).

Experimental design

Determination of optimum conditions of HSDS

Determining the optimum conditions for HSDS was conducted in two experimental sections: (1) experiment 1.1, determining the optimum feed water flow rate; and (2) experiment 1.2, determining the optimum initial feed water concentration. Both experiments were conducted in a semi-batch manner, with a feed water volume of 20 liters, an operating pressure of 70 mbar, and a cooling water flow rate of 1 L/minute.

In experiment 1.1, feed water with an initial concentration of 10 g/L was fed into the evaporator at a flow rate varying between 0 and 50 ml/minute. Then, several key parameters were measured periodically every 60 minutes for a 5-hour period: solar irradiance, temperature in each subunit, condensate volume, and product water quality parameters (salinity, total dissolved solid, pH,

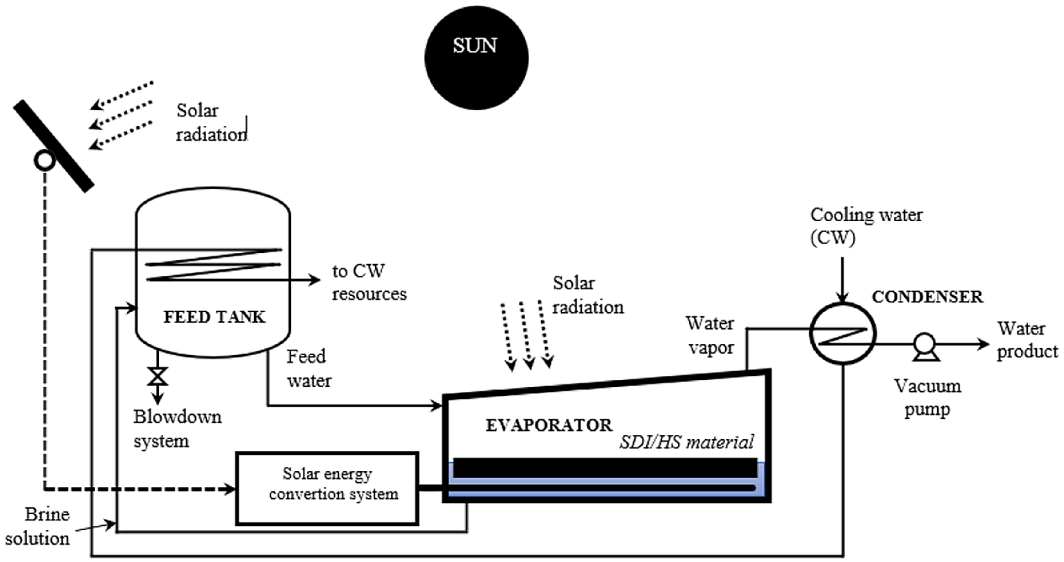

Figure 1. Developed innovative hybrid solar desalination system (HSDS)

and turbidity). All these parameters were measured by three replications. In experiment 1.2, feed water with initial concentration variation between 10–35 g/L, flowed into the evaporator flow rate of the optimum discharge in experiment 1.1. Then, several key parameters were measured periodically every 60 minutes within a period of 5 hours, namely: solar irradiance, temperature in each sub-unit, condensate volume, and water product quality parameters. Measurement of these parameters was carried out in 3 replications.

Determination of HSDS performance

The HSDS system performance study was conducted in a semi-batch manner, consisting of two experimental sections: (1) experiment 2.1, determining the effect of using SDI/HS materials, namely the materials that accelerate evaporation on the surface (solar-driven interface) or materials that store heat (thermal energy storage), and (2) experiment 2.2, determining the optimum cooling water flow rate; both experiments were conducted with a feed water volume of 20 liters, an operating pressure of 70 mbar, and the optimum flow rate and initial concentration of the feed water in experiment (1).

Experiment 2.1 was conducted using the optimum conditions of experiments (1), using three variations of SDI/HS materials: black gravel, black sand, and river (quartz) sand. The SDI/HS material was placed in the evaporator in two different placement options: (1) filled directly into the evaporation chamber, and (2) floated in the liquid filling the evaporator using a perforated tray structured as shown in Figure 2. The filling option that yielded the optimum results was then used in experiment 2.2. As in the previous experiment, several key parameters were measured periodically every 60 minutes over a 5-hour period: solar irradiance, temperature in each sub-unit, condensate volume, and water product quality parameters including salinity, total dissolved solids (TDS), pH, and turbidity. All these parameters were also measured in 3 replications.

Experiment 2.2 was conducted with several variations in cooling water flow rates between 1–4 L/minute, with the feed water flowing at the optimum flow rate and initial concentration of the feed water in experiment (1). Then, several key parameters were measured periodically every 60 minutes for a 5-hour period, including: solar irradiance, temperature in each sub-unit, condensate volume,

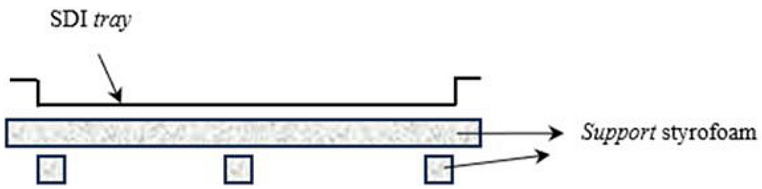

Figure 2. Tray for 2nd filling option of the SDI/HS material

and product water quality. Measurement of these parameters was carried out in 3 replications.

Analysis of variance (ANOVA)

In order to obtain conclusions regarding the effect of the use of SDI/HS materials on the performance of the HSDS, as well as the effect of the interaction between the time variable and the type of material, the experimental data were analyzed by using the 2-way ANOVA statistical method.

RESULT AND DISCUSSION

The research began with the fabrication of desalination equipment and the installation of a solar energy conversion system. The desalination equipment developed uses a hybrid heating system (direct and indirect heating), consisting of four main units: a feed tank, evaporator, condenser, and condensate tank. The desalination equipment was mounted on a support system that allowed for easy movement according to operational and mobility requirements (Figure 3).

Unlike conventional solar still systems, and the systems used by previous researchers such as Isah et al. (2022), Abd Elbar and Hassan, (2020b), Munawar et al., (2022), and El Mousssaoui et al., (2021), the HSDS system used has a separate condensation unit, as well as a feed tank designed to accommodate a heat recovery system with a feed water recycling system and cooling water return from the condenser through tubes. The HSDS system was also equipped with a vacuum system, a feed water recycling system, and uses a solar driven interface (SDI) or heat storage (HS) material, which aimed to improve the overall performance of the system. The combination of a two-way heating system, a vacuum system, the use of SDI/HS material, and a heat recovery system in one integrated system is a new innovation in the solar still system that is being used for the first time in this study.

The supporting system for indirect heating is a solar energy supply system (photovoltaic), which consists of 18 integrated solar panels, an AC-DC inverter, and a current storage battery, which has a maximum electrical energy supply capacity of 1800 W (Figure 4). This system supplies the energy needs for heating in a solar desalination system (HSDS) with a power of 1000 W. Such a system has its own advantages, namely allowing electrical energy storage in the battery during the day, thus enabling the use of electrical energy at night.

While the use of solar energy conversion systems has significant potential to reduce the energy costs in thermal desalination systems, their implementation requires a relatively large initial investment. Furthermore, these systems require proper maintenance to avoid problems such as short circuits, corrosion, and environmental damage. If all systems supporting the desalination process could utilize the electrical energy from solar energy conversion systems, the system would be able to operate at very low costs, as the energy would be available free of charge.

Optimum system condition

The optimum conditions of the HSDS system were determined with several variations in feed

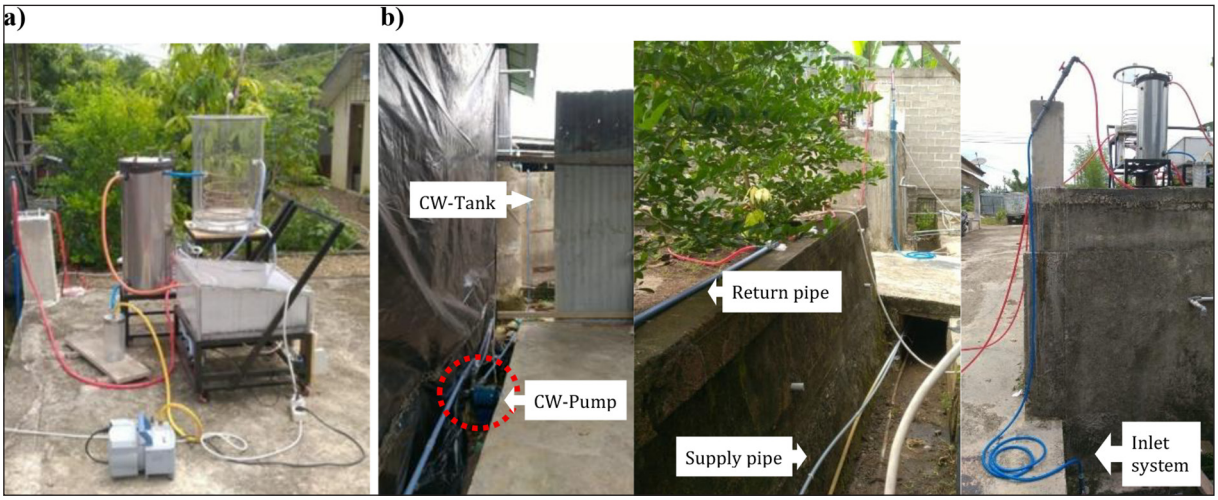

Figure 3. (a) Developed hybrid solar desalination system, (b) cooling water system

Figure 4. Solar energy conversion system (PV system): (a) solar panels; (b) control panels

flow rate, cooling water, and feed concentration as described in section 2.4. The volume of the condensate produced by HSDS was inversely proportional to the feed water flow rate. The higher the solution flow rate, the lower the condensate volume produced (Figure 5a). The optimum condensate volume was obtained under batch conditions (flow rate 0) which produced 2974 ml of freshwater. The production flux (5-hourly yield) for batch conditions was quite high, reaching 11.9 L/m^2 (Figure 5b). Under continuous conditions, the system's production flux reached 10.42 L/m^2 obtained at flow rate of 42.0 ml/min. These data confirmed that the HSDS has a potential of optimum daily yield of 50 to 57.1 L/m^2.day under continuous and batch conditions, respectively. As a comparison, these data were quite high compared to the yield reported by several previous researchers, such as Isah et al. (2022a), Munawar et al. (2022), and Abd. Elbar and Hassan (2020) with yields of 19.7 L/m^2.day, 18.5 L/m^2.day, and 3.5 kg/m^2.day, respectively. The initial feedwater concentration has the same effect as the flow rate, where the higher the initial feedwater concentration, the lower the volume of condensate produced (Figure 6a). This is closely related to the colligative properties of solutions, where the solutions with high concentrations will experience an increase in boiling point compared to their dilute counterparts (Elsayed et al., 2021). On the other hand, according to Al-Shammiri (2002), an increase in the initial concentration will lower the vapor pressure at the liquid surface, thereby decreasing the evaporation rate. Similarly, Sharqawy et al. (2010) stated that evaporation in an evaporator is a function of salinity and temperature.

In a batch system, evaporation slows down as the brine concentration increases. However, in a continuous system, a flow rate that is too high also has the potential to reduce the evaporation rate due to mixing that is too fast, which causes the temperature of the solution in the system to decrease. The optimum condensate volume is 2817 mL, obtained at an initial concentration of 10 g/L.

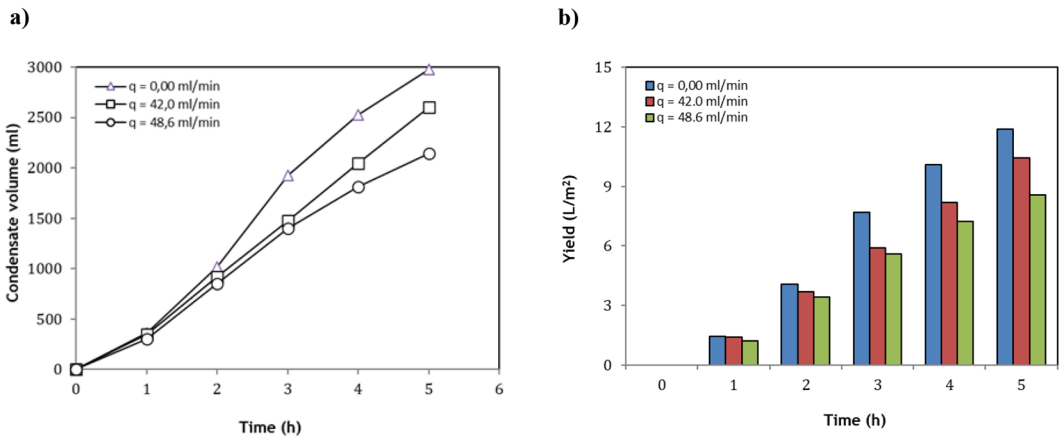

Figure 5. (a) Condensate volume, (b) hourly yield at various flowrate of feed water

The highest 5-hourly yield at this initial concentration variation was 11.7 L/m^2 (Figure 6b), quite close (around 5.3%), below the optimum yield in the previous feedwater flowrate determination experiment. This data indicated the daily potential yield of 54.1 L/m^2.

Improvement of HSDS performance

The performance of a thermal desalination system is largely determined by the performance of its two main units: the evaporation unit and the condensation unit. In this study, the performance of the evaporation unit was improved by using a two-way heating system, a vacuum system, a heat recovery system, and the use of solar driven interface (SDI) or thermal energy storage materials to increase surface area and function as heat storage (HS) materials. Meanwhile, the condensation system used variations in the cooling water flow rate to achieve optimum steam condensation in the condenser.

The use of SDI/HS material

The performance of HSDS has been improved using the materials that increase the evaporation surface area by using the SDI or HS material. The materials used were black gravel, black sand, and quartz sand. Initially, the SDI/HS material was placed directly in the evaporation chamber, and for comparison, it was then floated in the liquid by placing it in a perforated tray (Figure 7).

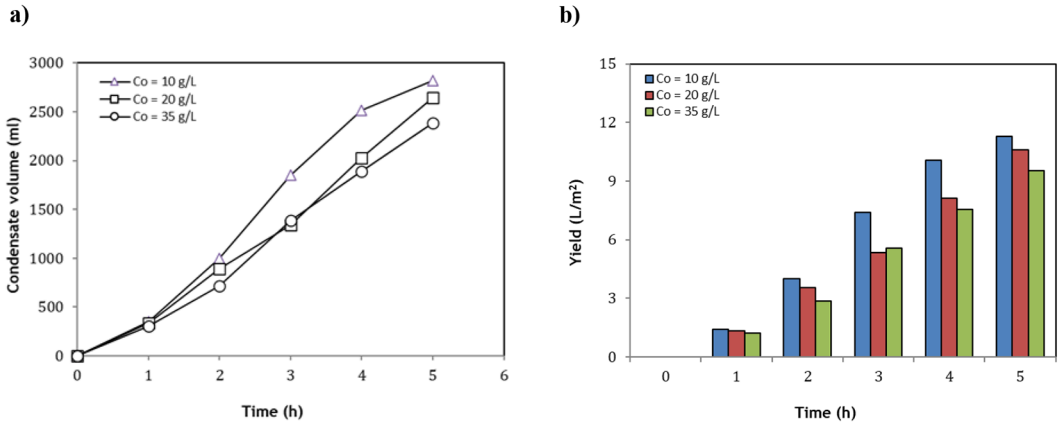

Figure 6. Effect of feed water concentration to: (a) condensate volume, (b) hourly yield

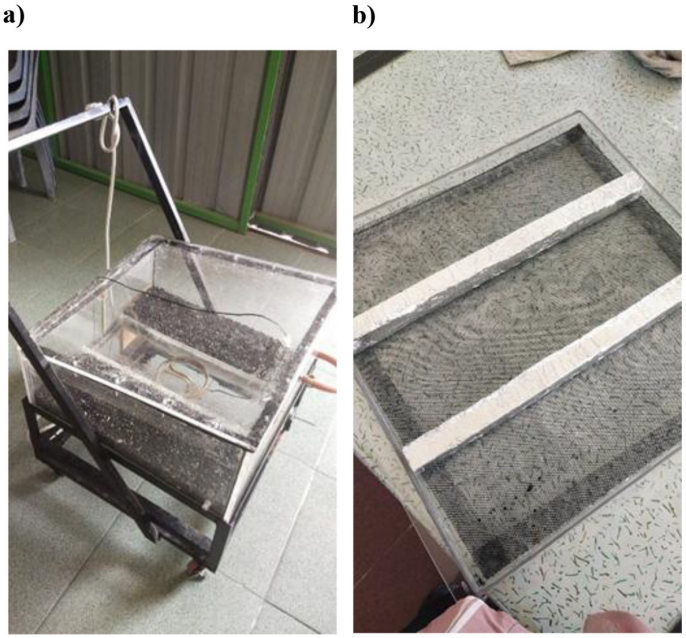

Figure 7. SDI/HS material placement options in the evaporator: (a) direct, (b) on tray

The use of trays for the SDI/HS material apparently has an unfavorable effect on HSDS performance. The experiments with black sand showed that when filled directly into the evaporator, the production rate was in the range of 722–785 ml/hour, but decreased significantly to between 420–576 ml/hour when the SDI/HS tray was used (Figure 8). The decrease in production rate when using trays is thought to occur because some of the vapor is retained at the bottom of the tray, which then condenses in the evaporator, thereby reducing the steam supply and the condensation rate in the condenser unit.

The effect of using SDI/HS materials in the evaporator directly was shown in Figure 9a. The three SDI materials used, namely black gravel, quartz sand, and black sand, showed quite good performance, producing condensate of 4754 ml, 3975 ml, and 3795 ml, respectively. The 5-hourly yields were 19.02, 15.9, and 15.18 L/m^2 respectively. This means that the potential daily production flux of the three materials is 91.3 L/m^2, 76.3 L/m^2, and 72.9 L/m^2 respectively (Figure 9b). These data indicate that black gravel is a better SDI/HS material compared to quartz sand and black sand.

These results are consistent with those reported by Nema et al. (2025) who compared the use of black-painted gravel aggregate and silica sand as thermal energy storage materials in a conventional solar still. The study, which used a solar still with a surface area of 0.5 m^2, reported an increase in optimum yield of 131.25%, with a total flux of 2.59 liters after 12 hours of operation, obtained when using black-painted gravel aggregate.

If the solar still with TEMS addition developed by Nema et al. (2025) was used as a comparison to the HSDS system used in this study, it would be identified that the use of a direct and

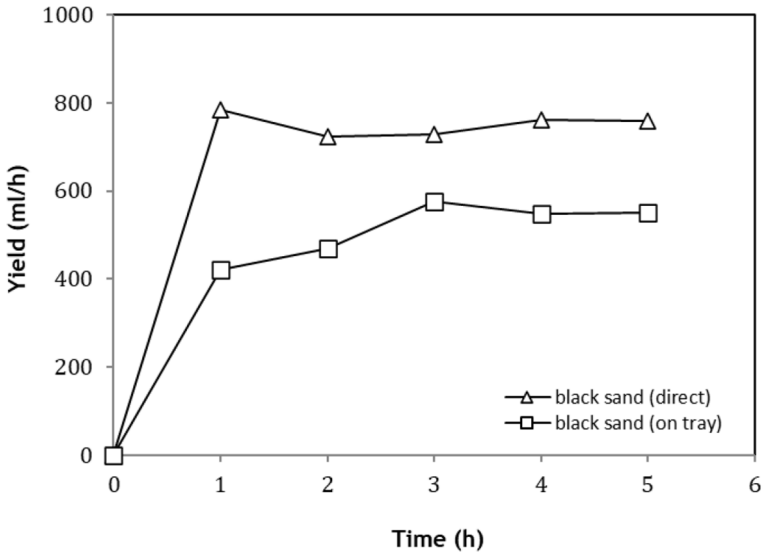

Figure 8. The effect of the SDI/HS filling method on the condensate production rate

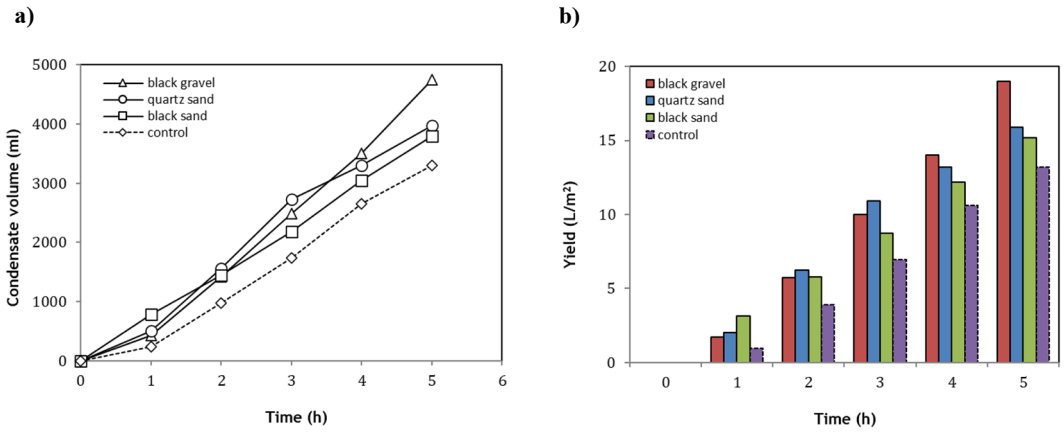

Figure 9. The effect of the SDI/HS material on the: (a) condensate volume, (b) hourly yield

indirect heating, a vacuum system, and SDI/HS materials such as black gravel, has a good performance to give a significant impact to enhance the desalination system performance. Daily performance enhancement was above 180% compared to their system.

Laboratory experiments have shown that as a heat storage material, black gravel can still produce a yield of approximately 428 ml for a cross-sectional area of 0.25 m^2 under the conditions of decreasing irradiance from 1552 to 362.5 W/m^2. However, because it is used under the conditions of high salinity and temperature, like rocks in general, gravel has the potential to experience weathering after prolonged use (Nahhas et al., 2019; Oguchi and Yu, 2021). Weathering usually occurs based on the mechanisms of salt crystallization within the pores, chemical reactions between brine and basalt minerals, or thermal cycling (Oguchi and Yu, 2021; Zhang et al., 2015). Technically, rock weathering in high-salinity and high-temperature environments can be significantly slowed down by several methods, including selecting low-porosity rocks, using hydrophobic or impermeable coatings to inhibit salt penetration (Andreotti et al., 2019; Lucero et al., 2025), controlling temperature fluctuations during system operation, and periodically cleaning the TES material to remove salt accumulation. These approaches can collectively extend the life of the material even in aggressive environments. From another perspective, the effects of each SDI/HS material appear very different (Figure 9), making it difficult to draw general conclusions. Therefore, the experimental data need to be analyzed statistically using a 2-way ANOVA model with interaction. Mathematical model is expressed as:

$$Y_{ijk} = \mu + \alpha_i + \beta_j + (\alpha\beta)_{ij} + \varepsilon_{ijk} \quad (1)$$

Assuming $\varepsilon_{ijk} \sim N(0,\sigma^2)$, independent. Referring to the experimental design, the research design of the effect of using SDI/HS materials is a 3 × 5 factorial experiment with 3 replications. The hypotheses tested in the ANOVA analysis were: (1) H_o: There is no impact of variables (time, type of materials) and interaction between its to production rate of condensate, and; (2) H_1: There is an impact of variables (time, type of materials) and interaction between its to production rate of condensate. The results of ANOVA are summarized in Table 1. The results of ANOVA show that factor A (time) giving F ≃ 30490178, higher than the F_{crit} (α =0.01) ≃ 4.02, indicating a significant influence on the condensate production rate. Factor B (materials) giving F ≃ 463593, higher than the F_{crit} (α =0.01) ≃ 5.39, also indicating a significant influence on the condensate production rate, as well as interaction A×B that giving F ≃ 417518, higher than the F_{crit} (α =0.01) ≃ 3.17. Factor A contributes more than 97.19% impact on condensate production rate, compared to 1.48% and 1.33% contribution of factor B (type of material) and A×B interaction, respectively.

Effect of cooling water flowrate

The cooling water flow rate has a significant effect on production flux. Data trends confirm that the product volume increases directly with cooling water flow rate (Figure 10a). The optimum 5-hourly yield obtained was 28.03 L/m^2 (Figure 10b), which was produced at a flow rate of 4 L/minute, and almost 3-fold increase compared to the flux at a flow rate of 1 L of cooling water/minute. These results illustrate that the developed HSDS has a fairly high daily yield potential when compared to previous studies, including those by Isah et al. (2022a), Munawar et al. (2022), Abd Elbar and Hassan (2020b), and Iqbal et al. (2024), who reported the daily flux of 19.7 L/m^2.d, 18.5 L/m^2.d, 3.5 kg/m^2.d, 8.3 L/m^2.d, respectively. These data show that the developed innovative HSDS having a good potential for further development.

These results are considered quite realistic, considering that the condensation of water vapor in the condenser is largely determined by the quantity of cooling water mass that serves to lower the

Table 1. ANOVA calculation summary

Source of variation	Sum of square (SS)	Degree of freedom (df)	Mean square (MS)	F
Factor A (time)	73176427	4	18294107	30490178
Factor B (type of material)	556312	2	278156	463593
Interaction A×B	2004086	8	250511	417518
Error (SSE)	18	30	0.6	-
Total	75736843	44	-	-

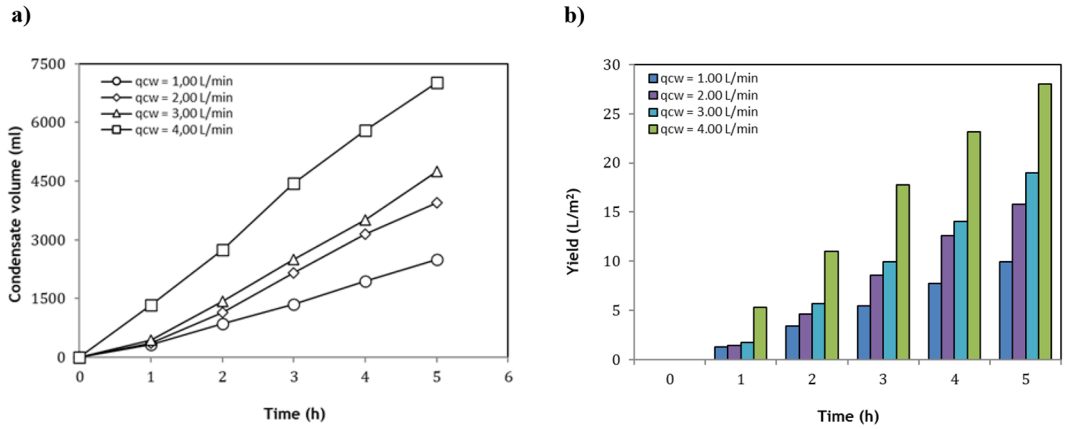

Figure 10. The effect of cooling water flowrate on the: (a) condensate volume, (b) hourly yield

temperature of the vapor until it reaches its dew point. Similar phenomena have been reported by several previous researchers, such as Attia (2015), Larboui et al. (2024), Smith et al. (2024), who showed that the condensation process is greatly influenced by the cooling water flow rate, cooling temperature, and condenser configuration.

The configuration of the steam (hot fluid) and cooling water (cold fluid) flow direction in the condenser also affects the condensation rate (Figure 11). The application of countercurrent flow produces a higher flux, which indicates that condensation takes place better if the countercurrent flow configuration is used. In counterflow or countercurrent flow, the temperature difference (ΔT) distribution between the steam and cooling water remains larger and more even throughout the condenser, thus encouraging a higher heat transfer rate, and increasing condensation efficiency. Meanwhile, in the concurrent flow configuration, the temperatures of the hot and cold fluid streams meet more quickly, thus encouraging the initial condensation rate, but decreasing the temperature gradient over time, which causes a decrease in the overall condensation rate.

Energy analysis

The performance of the desalination system was analyzed in terms of thermal efficiency, expressed as the Gain Output Ratio (GOR), which represents how much production capacity can be generated from a given amount of heat energy supplied to the desalination system. The GOR was analyzed by using Equation 2 (Elhenawy, 2022):

$$GOR = \frac{m_C L_V}{Q_i} \quad (2)$$

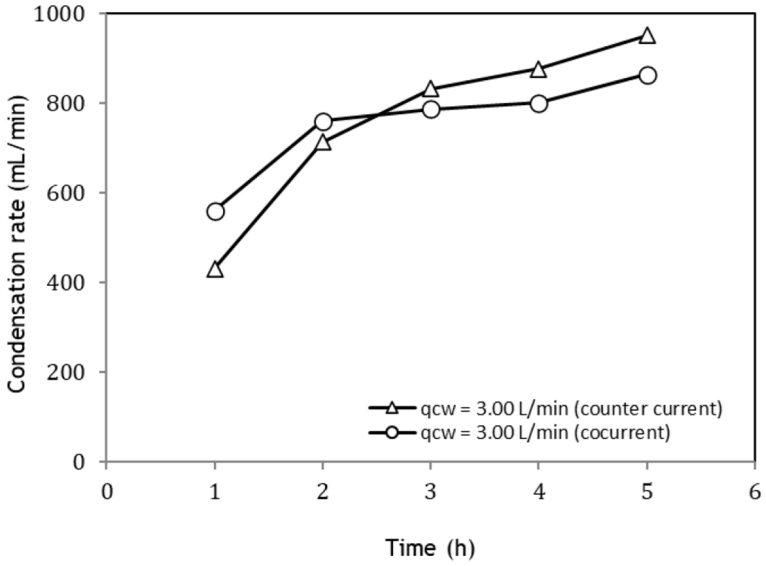

Figure 11. The effect of fluid flow direction on condensation rate

where: m_c – mass of condensate, L_V – latent heat of vaporization, Q_i – input energy to the evaporation system.

In order to obtain the GOR value, it is necessary to calculate the energy entering the desalination system, E_i. Referring to the energy balance, the general equation of the heat balance can be expressed in the form:

$$E_i = Q_c + Q_{Loss,E} \quad (3)$$

where: Q_C – consumption of energy in the system, and $Q_{loss,E}$ – losses of energy from the system.

Since the input energy comes from solar heat, heaters, and electrical energy for vacuum pumps and liquid pumps, the E_i that enters the system are:

$$E_i = Q_{SS} + Q_{SH} + E_{VP} + E_{WP} = Q_i + E_{VP} + E_{WP} \quad (4)$$

where: Q_{SS} – heat from solar light, Q_{SH} – heat from solar heater, E_{VP} – energy used by vacuum pump, E_{WP} – energy used by cooling water pump.

The heat from sunlight (Q_{ss}) can be calculated by using Equation 5:

$$Q_{SS} = IA_E t \quad (5)$$

where: I – solar irradiance (W/m^2), A_E – cross-sectional area of evaporator (m^2), and t – operating time (s).

The heat from the solar heater (Q_{SH}) can be calculated using Equations 6 and 7:

$$I = \frac{Lux}{120} \quad (6)$$

and:

$$Q_{SH} = hA_h(T_{SH} - T_B) \quad (7)$$

where: Q_{SH} – heat from solar heater, h – convective heat transfer coefficient, A_H – cross-sectional area of heater, T_{SH} – temperature of solar heater, T_B – temperature of brine.

Meanwhile, the energy consumption in the system (Q_c) is the energy for evaporation of liquid in the evaporator, which can be expressed by Equation 8:

$$Q_c = m_V L_V + Q_B \quad (8)$$

where: m_V – mass of vapor, Q_B – heat of brine.

The latent heat of vaporization, and sensible heat of vaporization can be calculated using Equations 9 and 10:

$$L_V = 2501{,}9 - 2.41T + 0.0012T^2 - 0.000016T^3 \quad (9)$$

and:

$$Q_B = m_B C_p (T_B - T_{FW}) \quad (10)$$

where: m_B – mass of brine, C_p – heat capacity of water, T_B – temperature of brine, and T_{FW} – temperature of feed water.

The energy requirements for the vacuum pump (E_{VP}), and the cooling water pump (E_{WP}), since both are electric pumps, can be calculated using Equation 11:

$$E_P = P \cdot t \quad (11)$$

where: E_p – the pump work (J), P – the pump power, and t – the operating time (s).

The pump power for 1-phase alternating current can be calculated using Equation 12:

$$P = V \cdot I \cdot f_p \quad (12)$$

where: V – voltage (V); I – current (A), and; fp – power factor (for pumps: fp = 0.7–0.9).

Using the energy balance principle, heat loss ($Q_{loss,E}$) can be calculated from the input energy data (E_i), energy consumption in the system (Q_c), and pump energy (E_{VP}, E_{WP}) using Equation 13:

$$Q_{Loss,E} = E_i - Q_c - E_{VP} - E_{WP} \quad (13)$$

The results of heat calculation of E_i, Q_c, $Q_{loss,}$ are displayed in Figure 12. The energy supplied to the system ranges from 13,064–15,506 kJ, with an energy consumption of 9,415–9,601 kJ. Meanwhile, energy loss within the system was 3,463–6,091 kJ, or approximately 26.51–39.28% of the energy supplied to the system. This amount of energy loss was quite reasonable, considering that the developed system does not use thermal insulation yet. Calculation of Gain output ratio (GOR) giving an optimum result of 1.32, obtained at cooling flowrate of 4 L/minutes.

On the one hand, this condition indicates that thermal insulation has not been optimally utilized in the developed desalination system. However, on the other hand, it indicates that system performance can still be improved, also by reducing the energy losses within the system. Several system improvements, such as the use of thermal insulation (Khalifa and Hamood, 2009; Muthu Manokar et al., 2020), conditioning the evaporator as a

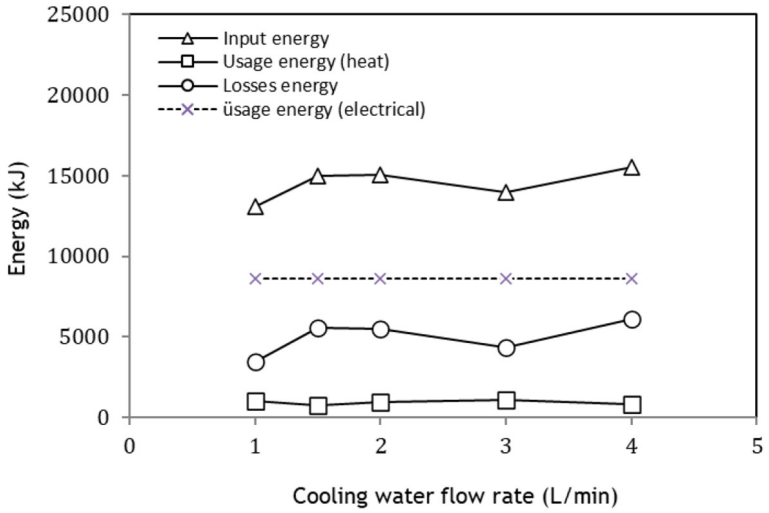

Figure 12. Input, usage, and losses of energy at various cooling water flowrate

thermal absorber (Manchanda and Kumar, 2015; Sahoo et al., 2008), and optimizing the heat recovery system, are estimated to be effective solutions to reduce energy losses and improve system performance. The use of thermal insulation with the right thickness (30–60 mm) and the use of black color on the inside of the evaporator effectively reduces energy loss and increases thermal efficiency between 2.5–80% (Manchanda and Kumar, 2015; Muthu Manokar et al., 2020; Sahoo et al., 2008; Tony and Nabwey, 2024) compared to the system without insulation. Thermal insulation reduces the rate of heat transfer by conduction and convection from structural elements that do not directly contribute to evaporation, so that more thermal energy can be used to maintain high water temperatures and accelerate evaporation.

The performance of the desalination system also analyzed based on the mass and energy balance calculation data. Besides GOR, three parameters were used, namely, thermal efficiency (E_T) production yield (E_D), condensation efficiency (E_C), calculated using Equation 14, 15 and 16:

$$E_T = \frac{m_C L_V}{E_i} \times 100\% \quad (14)$$

$$E_D = \frac{m_C}{m_{FW}} \times 100\% \quad (15)$$

$$E_C = \frac{F_C . t}{M_V} \times 100\% \quad (16)$$

where: m_{FW} mass of feed water, and F_C mass flow of condensate.

The results of efficiency analysis are shown in Figure 13. The calculation results show that the

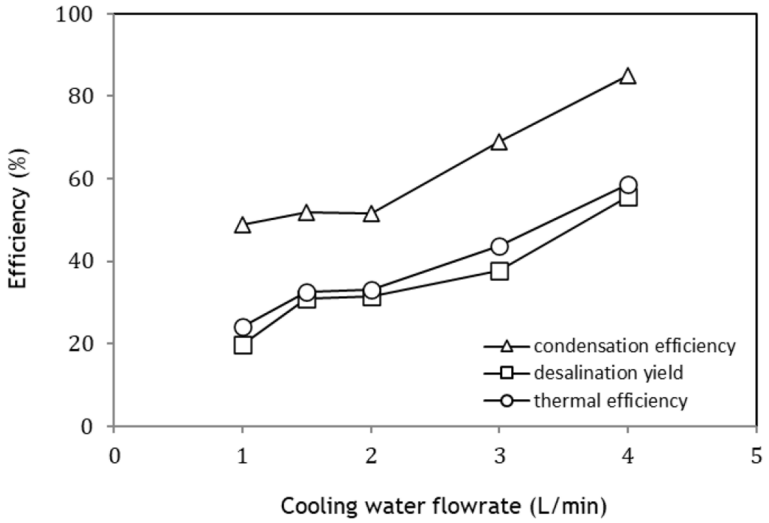

Figure 13. Key performance of developed HSDS at various cooling water flowrate

Table 2. Comparison of performance between the developed HSDS with recent another solar desalination system

Typical of solar desalination system	Specification	Key performance			Authors
		Yield	Units	Thermal efficiency, %	
Rectangular solar still	Used preheating system, and black steel wool fibers	3.53	kg/m^2.d	38.1	Abd Elbar and Hassan (2020)
Floating solar still	Used a hydrophilic solar-absorbing layer above floating polystyrene foam	3.90	L/m^2.d	40.3	Xu et al. (2020)
Tubular solar still	Used parabolic concentrator solar tracking system	4.27	L/m^2.d	32.4	Alhadri et al. (2022)
Interfacial solar still	Used corrugated wick, barrel wick, flat wick, and conventional solar still	4.40	L/m^2.d	48.5	Younes et al. (2021)
Hemispherical solar still	Added cotton fabric, nanofluid, pure and nano-based PCMs; used rubber insulation	5.05	L/m^2.d	45.6	Sharshir et al. (2023)
Tubular solar still	Novel double-effect tubular solar still with concentrated sunrays	5.20	L/m^2.d	40.4	Ahmed et al. (2021)
Tubular solar still	Used PVC, PC, acrylic, glass cover	6.23	L/m^2.d	71.6	Sambare et al. (2022)
Tubular solar still	Used waste plastic bottles with black cotton wick	6.83	L/m^2.d	58.5	Elashmawy et al. (2024)
Tubular solar still	Tubular solar still with half two concentric cylinders and CPC	7.48	L/m^2.d	61.4	Kabeel et al. (2020)
Rectangular solar still	Added silica sand and black gravel as TESM materials	2.59	L/ m^2.12h	N/A	Nema et al. (2025)
Rectangular solar still	Optimized design parameters incl. glass cover & insulation thickness, W/L ratio; used winding flow to enhance detention time	2.78	L/m^2.8h	N/A	Iqbal et al. (2024)
Rectangular hybrid solar still	Used solar radiation, PV system, and combination of solar-PV as a heat resources	24.30	L/m^2.d	30.1	Isah et al. (2022b)
Rectangular hybrid solar still	Used solar-PV and vacuum system with separated condenser; used quartz sand, black sand, and black gravel as SDI/HS materials	28.03	L/m^2.5h	58.7	This study (2025)

desalination yield increases with increasing cooling water flow rate. The optimum desalination yield was 55.42%, which was achieved at a feed flow rate of 42 ml/min, an initial concentration of 10 g/L, and a cooling water flow rate of 4 L/min, and the use of black gravel as the SDI/HS material. The maximum steam condensation efficiency under the same conditions was 84.98%, meanwhile the optimum thermal efficiency was 58.7%, respectively.

Condensation efficiency is influenced by several factors, including the cooling water flow rate, heat transfer surface area, condenser configuration, fluid flow direction, including the use of a vacuum system in the desalination system. The experiments on concurrent flow resulted in a lower condensation efficiency of 64.67% (Figure 11), indicating that the configuration of hot and cold fluid flows in the condenser also has an effect on condensation efficiency.

Several researchers, including Smith et al. (2024) and Attia (2015), have shown that increasing the cooling water flow rate results in a higher Reynolds number, thus generally increasing the overall heat transfer coefficient (U) and accelerating the release of condensation heat. This increases the condensation rate, provided that the condenser inlet temperature is sufficiently low, as the cooling temperature is also a determining variable (Larboui et al., 2024).

In line with desalination efficiency, under optimum conditions of the developed HSDS, the thermal efficiency increased along with cooling water flow rate. The thermal efficiency of HSDS was quite competitive when compared to several previous systems. Abd Elbar and Hassan (2020b), for example, reported a thermal efficiency of 38.07% for a hybrid desalination system consisting of solar panels, a solar still, porous materials, and a brine heater. Another study by Isah et al. (2022) using a hybrid system based on solar

Table 3. Water product quality

Parameters	Quality	Standard*	
	Initial	Final	
Salinity, mg/L	10,057	36.0	<300.0
TDS, mg/L	10,077	36.0	<300.0
Turbidity, NTU	8.70	8.50	<3.0
pH	7.58	8.11	6.5–8.5

Note: *Indonesian Minister of Health Regulation, No. 2, 2023.

panels and a solar still reported a thermal efficiency of 30.07%. The comparison of yield and thermal efficiency between the developed innovative HSDS with several reported solar desalination systems was shown in Table 2.

The yield obtained in the developed HSDS system was quite high, compared to previous studies, so it is quite difficult to maintain this performance in a scale-up system. However, according to the technical perspective, there are several options that can be recommended to maintain system performance, including maintaining the use of a vacuum system, optimizing heat recovery, and using a modular system or a multi-effect modular engineering approach. Technically, about 20–40% performance drop is typical during initial scale-up. If the design is not modular and heat recovery is not provided, the performance drop can be over 50%. All results obtained in this study were obtained under summer conditions in Lhokseumawe City, Aceh, Indonesia, during the period of March to August 2025. The differences in results may be obtained in other seasons due to differences in meteorological parameters including solar radiation, ambient temperature, wind speed, and humidity. During the desalination experiment period, the parameters of solar radiation, ambient temperature, wind speed, and humidity were obtained in the range of 995–1.538 W/m^2, 31–33 °C, 2–3 m/s, and 80–95%, respectively. In the rainy season, all these parameters were on average in the range of 200–1.000 W/m^2, 25–29 °C, 4–14 km/h, and 85–100%, respectively. These meteorological data confirm the logical consequence of the decreased performance of HSDS under lower solar radiation in the rainy season.

Improvement of water product quality

Salinity reduction in the HSDS desalination system is classified as very high, with an average removal efficiency above 99%. The final salinity concentration is 36 mg/L, thus meeting the drinking water quality standards referred to in the Indonesian Minister of Health Regulation, No. 2 of 2023. Likewise, other parameters such as TDS, pH, have met the quality standards (Table 3). However, the turbidity parameter is still above the quality standard value, which requires turbidity below 3 mg/L. System improvement is certainly still needed, if the condensate is to be used as a drinking water product.

The condition of high turbidity in desalinated water usually caused by several external factors, including the entry of suspended solid particles into the condensate, evaporation of volatile organic compounds (VOCs), recontamination after condensation, unfiltered colloids and microparticles, as well as desalination equipment design factors. Although the desalination process involves evaporation and condensation, imperfect operating mechanisms can cause micro-particles from the source water to be carried into the condenser. The splashing mechanism (steam carrying small droplets) in the evaporator can carry suspended particles, decomposing materials, or solid waste into the condensate if the cooling process is inefficient. In another case, some contaminants with boiling points close to or lower than water can also evaporate and then condense with the water, causing turbidity or color. Sometimes, after the steam is condensed, cross-contamination on pipe surfaces, storage tanks, or through ambient air, such as dust or organic aerosols, can cause particles to enter the water. The evaporation process was not always effective in removing all colloidal particles or small particles in the liquid phase, especially if there are mechanical disturbances such as vibration and turbulence. According to design aspect, device leaks, temperature fluctuations, or inefficient condenser design can cause variations in electrochemical or microscopic features in the condensate. This additional turbidity can be prevented by using a tightly closed desalination system, regular condenser cleaning, and using a sterile condensate container. In the case of turbidity remains high, polish treatment of the condensate by using microfiltration or activated carbon can be an effective solution.

CONCLUSIONS

The performance of innovative HSDS was determined. The data of the optimum conditions and performance of the HSDS desalination system

have been obtained. The performance of the developed HSDS desalination system is quite high, with hourly yield of 28.03 L/m^2 over 5 hours, and the optimum desalination efficiency of 55.42%, which was obtained at a feed water flow of 42 mL/minute, a feed water concentration of 10 g/L, a cooling water flow of 4 L/minute, and the use of black gravel as SDI/HS material. The energy supplied to the system ranges from 13,064–15,506 kJ, with an energy consumption of 9,415–9,601 kJ. Meanwhile, the energy loss within the system was 3,463–6,091 kJ, or approximately 26.51–39.28% of the energy supplied to the system. Under optimum conditions, the thermal efficiency of HSDS was 58.7%, and gaining output ratio was 1.32. Improvement for the developed HSDS system is still needed, considering that the quality of the product water produced still does not meet the drinking water standards based on the Indonesian Minister of Health Regulation No. 2 years 2023, especially for turbidity parameters.

Acknowledgements

We would like to thank to the supported in part from the Institut Teknologi Bandung (ITB) for the research allowance, and the enabling environment, services, and support.

REFERENCES

1. Abd Elbar, A.R., Hassan, H. (2020). Enhancement of hybrid solar desalination system composed of solar panel and solar still by using porous material and saline water preheating, *Solar Energy*, *204*, 382–394. https://doi.org/10.1016/j.solener.2020.04.058
2. Abd Elbar, A.R., Hassan, H. (2020). Energy, exergy and environmental assessment of solar still with solar panel enhanced by porous material and saline water preheating, *Journal of Cleaner Production,* 277, 124175. https://doi.org/https://doi.org/10.1016/j.jclepro.2020.124175
3. Ahmed, M.M.Z., Alshammari, F., Abdullah, A.S., Elashmawy, M. (2021). Enhancing tubular solar still performance using double effect with direct sunrays concentration, *Solar Energy Materials and Solar Cells*, *230*. https://doi.org/10.1016/j.solmat.2021.111214
4. Alhadri, M., Alatawi, I., Alshammari, F., Haleem, M.A., Heniegal, A.M.A., Abdelaziz, G.B., Ahmed, M.M.Z., Alqsair, U.F., Kabeel, A.E., Elashmawy, M. (2022). Design of a low-cost parabolic concentrator solar tracking system: tubular solar still application, *Journal of Solar Energy Engineering, 144*. https://doi.org/10.1115/1.4054232
5. Alhaj, M., Tahir, F., Al-Ghamdi, S.G. (2022). Life-cycle environmental assessment of solar-driven multi-effect desalination (MED) plant, *Desalination, 524.* https://doi.org/10.1016/j.desal.2021. 115451
6. Al-Shammiri, M. (2002). Evaporation rate as a function of water salinity, *Desalination, 150,* 189–203. https://doi.org/10.1016/S0011-9164(02)00943-8
7. Anand, B., Shankar, R., Murugavelh, S., Rivera, W., Midhun Prasad, K., Nagarajan, R. (2021). A review on solar photovoltaic thermal integrated desalination technologies, *Renewable and Sustainable Energy Reviews, 141,* 110787. https://doi.org/10.1016/J.RSER.2021.110787
8. Andreotti, S., Franzoni, E., Ruiz-Agudo, E., Scherer, G.W., Fabbri, P., Sassoni, E., Rodriguez-Navarro, C. (2019). New polymer-based treatments for the prevention of damage by salt crystallization in stone, *Materials and Structures/Materiaux et Constructions*, *52*(1). https://doi.org/10.1617/s11527-018-1309-6
9. Attia, S.I. (2015). The influence of condenser cooling water temperature on the thermal efficiency of a nuclear power plant, *Annual Nuclear Energy*, *80*, 371–378. https://doi.org/10.1016/J.ANUCENE.2015.02.023
10. Bappenas, (2019). *Rencana Pengembangan Jangka Menengah Nasional 2020–2024*. https://www.bappenas.go.id/
11. Dong, Y., Tan, Y., Wang, K., Cai, Y., Li, J., Sonne, C., Li, C. (2022). Reviewing wood-based solar-driven interfacial evaporators for desalination, *Water Research, 223*, 119011. https://doi.org/10.1016/J.WATRES.2022.119011
12. El Moussaoui, N., Kassmi, K., Alexoupolos, S., Schwarzer, K., Chayeb, H., Bachiri, N. (2021). Simulation studies on a new innovative design of a hybrid solar distiller MSDH alimented with a thermal and photovoltaic energy, *Materials Today: Proceeding*, *45*, 7653–7660. https://doi.org/ 10.1016/j.matpr.2021.03.115
13. Elashmawy, M., Sharshir, S.W., Abdelaziz, G.B., Alshammari, F., Ahmed, M.M.Z., Soliman, A. M. (2024). Novel solar still design using transparent waste bottles, *Journal of Cleaner Production*, *434*, 140090. https://doi.org/10.1016/j.jclepro.2023.140090
14. Elhenawy, Y., Moustafa, G.H., Attia, A.M., Mansi, A.E., Majozi, T., Bassyouni, M. (2022). Performance enhancement of a hybrid multi effect evaporation/membrane distillation system driven by solar energy for desalination, *Journal of Environmental Chemical Engineering, 10,* 108855. https://doi.org/10.1016/J.JECE.2022.108855
15. Elsayed, M.L., Wu, W., Chow, L.C. (2021). High

salinity seawater boiling point elevation: Experimental verification, *Desalination, 504,* 114955. https://doi.org/10.1016/J.DESAL.2021. 114955

16. Fairuz, A., Faeshol Umam, M., Hasanuzzaman, M., Rahim, N.A., Mujtaba, I.M. (2023). Modeling and analysis of hybrid solar water desalination system for different scenarios in Indonesia, *Energy Conversion Management, 276,* 116475. https://doi.org/10.1016/ J.ENCONMAN.2022.116475
17. Iqbal, R., Aldrien Putra, D.R., Arifianingsih, N.N., Dwinandha, D. (2024). Evaluation of enhanced solar desalination system prototype, *Indonesian Journal of Urban and Environmental Technology, 7*, 151–163. https://doi.org/10.25105/urbanenvirotech.v7i2.20768
18. Isah, A.S., Bt Shafiai, S.H., Takaijudin, H.B., Singh, B.S.M., Gilani, S.I.U.H. (2022a). The role of desalination and contribution of hybrid solar desalination system towards primary health care, *Case Studies in Chemical and Environmental Engineering, 6,* 100253. https://doi.org/10.1016/ J.CSCEE.2022.100253
19. Isah, A.S., Bint Takaijudin, H., Singh, M., Singh, B., Gilani, S.I.U.H., Wan Yusof, K., Abdurrasheed, S., Abimbola, T.O., Shoeb, M.M. (2022b). Solar energy desalination distillate yield and cost evolution, and statistical relationship between meteorological variables and distillate yield, *Solar Energy, 246,* 256–272. https://doi.org/10.1016/j.solener.2022.09.025
20. Kabeel, A.E., Harby, K., Abdelgaied, M., Eisa, A., (2020). Performance of the modified tubular solar still integrated with cylindrical parabolic concentrators, *Solar Energy*, *204*, 181–189. https://doi.org/10.1016/j.solener.2020.04.080
21. Khalifa, A., Hamood. A. (2009). Effect of insulation thickness on the productivity of basin type solar stills: An experimental verification under local climate, *Energy Conversion and Management*, *50*(9), 2457–2461. https://doi.org/10.1016/j.enconman.2009.06.007
22. Kumar, S., Kumar, M., Chowdhury, S., Rajpurohit, B.S., Randhawa, J.K. (2022). Environmental concerns and long-term solutions for solar-powered water desalination, *Journal Cleaner Production, 345,* 131180. https://doi.org/10.1016/J.JCLEPRO.2022.131180
23. Larboui, K., Douani, M., Maouche, W., Tahri, T., Labbaci, A. (2024). The exergetic approach for the analysis of HDH desalination process using a pulverized column, *Desalination and Water Treatment, 317*, 100218. https://doi.org/10.1016/J.DWT.2024.100218
24. Li, H., Yan, Z., Li, Y., Hong, W. (2020). Latest development in salt removal from solar-driven interfacial saline water evaporators: Advanced strategies and challenges, *Water Research, 177,* 115770. https://doi.org/10.1016/J.WATRES.2020.115770
25. Lucero, R., Salisid, K., Oros, R., Bongabong, A., Alguno, A., Villacorte-Tabelin, M., Silwamba, M., Phengsaart, T., Tabelin, C. (2025). Nanosilica-based hybrid hydrophobic coatings for stone heritage conservation: An overview, *Minerals, 15(11)*, 1134. https://doi.org/10.3390/ min15111134
26. Manchanda, H., Kumar, M. (2015). A comprehensive decade review and analysis on designs and performance parameters of passive solar still, *Renewables: Wind, Water, and Solar, 2*(1). https://doi.org/10.1186/s40807-015-0019-8
27. Munawar, Majuar, E. (2019). The Biomass-based Desalinator Performance in a Vacuum System, *IOP Conference Series: Material Science Engineering, 536*, 012112. https://doi.org/10.1088/1757-899X/536/1/012112
28. Munawar, Sami, M., Fachraniah, Nasri, (2022). Produksi Kondensat pada Sistem Desalinasi Air Asin Berbasis Energi Surya, in: Prosiding Seminar Nasional Politeknik Negeri Lhokseumawe, Politeknik Negeri Lhokseumawe, A44–A48.
29. Muthu Manokar, A., Taamneh, Y., Kabeel, A., Prince Winston, D., Vijayabalan, P., Balaji, D., Sathyamurthy, R., Padmanaba Sundar, S., Mageshbabu, D. (2020). Effect of water depth and insulation on the productivity of an acrylic pyramid solar still – An experimental study, *Groundwater for Sustainable Development, 10*, 100319. https://doi.org/10.1016/J.GSD.2019. 100319
30. Nahhas, T., Py, X,, Sadiki, N. (2019). Experimental investigation of basalt rocks as storage material for high-temperature concentrated solar power plants, *Renewable and Sustainable Energy Reviews*, *110*, 226–235. https://doi.org/10.1016/j.rser.2019.04.060
31. Nema, A., Thakur, V.K., Singh, P., Gaur, M.K., Shrivastava, V., Ray, R. (2025). Performance assessment of passive solar still with different thermal energy storage materials, *Desalination Water Treatment, 323*, 101288. https://doi.org/10.1016/J.DWT.2025.101288
32. Oguchi, C., Yu, S. (2021). A review of theoretical salt weathering studies for stone heritage, *Progress in Earth and Planetary Science, 8*(1), 32. https://doi.org/10.1186/s40645-021-00414-x
33. Pistocchi, A., Bleninger, T., Breyer, C., Caldera, U., Dorati, C., Ganora, D., Millán, M.M., Paton, C., Poullis, D., Herrero, F.S., Sapiano, M., Semiat, R., Sommariva, C., Yuece, S., Zaragoza, G. (2020). Can seawater desalination be a win-win fix to our water cycle?, *Water Research, 182,* 115906. https://doi.org/10.1016/J.WATRES.2020.115906
34. Raihananda, F.A., Philander, E., Lauvandy, A.F., Soelaiman, T.A.F., Budiman, B.A., Juangsa, F.B., Sambegoro, P. (2021). Low-cost floating solar still for developing countries: Prototyping and heat-mass transfer analysis, *Results in Engineering*, *12*, 100300. https://doi.org/10.1016/ J.RINENG.2021.100300

35. Sahoo, B., Sahoo, N., Mahanta, P., Borbora, L., Kalita, P., Saha, U.K. (2008). Performance assessment of a solar still using blackened surface and thermocol insulation, *Renewable Energy, 33*(7), 1703–1708.
36. Sambare, R.K., Dewangan, S.K., Gupta, P.K., Joshi, S. (2022). Energy, exergy and economic analyses of tubular solar still with various transparent cover materials, *Process Safety and Environmental Protection*, *168*, 1101–1108. https://doi.org/10.1016/j.psep.2022.10.064
37. Sharshir, S.W., Omara, M.A., Joseph, A., Kandeal, A.W., Elsaid, A.M., El-Said, E.M.S., Alatawi, I., Elashmawy, M., Abdelaziz, G.B. (2023). Thermoenviroeconomic performance augmentation of solar desalination unit integrated with wick, nanofluid, and different nano-based energy storage materials, *Solar Energy*, *262*, 111896. https://doi.org/10.1016/j.solener.2023.111896
38. Sharqawy, M.H., Lienhard V, J.H., Zubair, S.M. (2010). Thermophysical properties of seawater: A review of existing correlations and data, *Desalination and Water Treatment, 16,* 354–380. https://doi.org/10.5004/dwt.2010.1079
39. Smith, H., Assagaf, M., Suwarda, R., Budiyanto, A., Adinegoro, H., Manalu, L.P., Rienoviar, Rosniati, Manoi, F., Loppies, J.E., Ramlah, S., Sunarmani, Widayanti, S.M., Setyadjit, Marwati, T., Setyawan, N., Tjahjohutomo, R., Syaefullah, E., Risfaheri, Bin Arif, A. (2024). The flow rate of the condenser cooling water in the distillation process increases the quality and quantity of patchouli oil, *Scientific World Journal*. https://doi.org/10.1155/2024/9844242
40. Subramani, A., Jacangelo, J.G. (2015). Emerging desalination technologies for water treatment: A critical review, *Water Research, 75*, 164–187. https://doi.org/10.1016/J.WATRES.2015.02.032
41. Tony, M., Nabwey, H. (2024). Recent advances in solar still technology for solar water desalination, *Applied Water Science, 14*(7), 147. https://doi.org/10.1007/s13201-024-02188-1
42. Younes, M.M., Abdullah, A.S., Essa, F.A., Omara, Z.M., Amro, M.I. M.I. (2021). Enhancing the wick solar still performance using half barrel and corrugated absorbers, *Process Safety and Environmental Protection*, *150*, 440–452. https://doi.org/10.1016/j.psep.2021.04.036
43. Xu, J., Wang, Z., Chang, C., Fu, B., Tao, P., Song, C., Shang, W., Deng, T. (2020). Solar-driven interfacial desalination for simultaneous freshwater and salt generation, *Desalination, 484,* 114423. https://doi.org/10.1016/j.desal.2020.114423
44. Zhang, R., Zhang, X., Hu, S. (2015). Basalt–water interactions at high temperatures: 1. Dissolution kinetic experiments of basalt in water and NaCl-H_2O at temperatures up to 400 °C, 23 MPa and implications, *Journal of Asian Earth Sciences*, *110,* 189–200. https://doi.org/10.1016/J.JSEAES. 2015.03.042